

**Lignin Monomer Conversion into Biolubricant Base Oils**

Journal:	<i>Green Chemistry</i>
Manuscript ID	GC-ART-09-2021-003350.R1
Article Type:	Paper
Date Submitted by the Author:	18-Oct-2021
Complete List of Authors:	Ebikade, Elvis; University of Delaware, Chemical and Biomolecular Engineering; University of Delaware, Chemical and Biomolecular Engineering Sadula, Sunitha; University of Delaware, Catalysis Center for Energy Innovation Liu, Sibao; Catalysis Center for Energy Innovation, Department of Chemical and Biomolecular Engineering; The University of Delaware Vlachos, Dion; Univ. of Delaware,

Lignin Monomer Conversion into Biolubricant Base Oils

Elvis Osamudiamhen Ebikade^{1,2}, Sunitha Sadula¹, Sibao Liu^{1,3}, and Dionisios G. Vlachos¹,

2*

¹Catalysis Center for Energy Innovation, University of Delaware, 221 Academy Street, Newark, DE, 19716 USA.

²Department of Chemical and Biomolecular Engineering, University of Delaware, 150 Academy Street, Newark, DE, 19716 USA.

³Key Laboratory for Green Chemical Technology of Ministry of Education, School of Chemical

Engineering and Technology, Tianjin University, Tianjin 300072, China

*Corresponding author: vlachos@udel.edu

Abstract

Despite progress in the depolymerization of lignin, only a few studies convert the obtained monomers to value-added products. Here we introduce a strategy to synthesize branched benzene lubricant (BBL) and branched cyclic lubricant (BCL) base oils from lignin-derived monomers and aldehyde. We perform carbon-carbon coupling via Brønsted acid-catalyzed hydroxyalkylation/alkylation (HAA) then hydrodeoxygenation (HDO). Optimum HAA reaction conditions achieve up to 90% guaiacol conversion and an HAA product containing 76% BBL and 24% enal condensation product over a P-SiO₂ catalyst. Subsequent HDO of HAA products over an Ir-ReOx/SiO₂ catalyst produces a lubricant-ranged mixture of BCL (C₂₄) up to yield (82%) and small fractions of dodecyl cyclohexane and C₁₀ and C₁₅ carbons alkanes. The kinematic viscosity, viscosity index, and Noack volatility of these base oils are comparable to commercial petroleum-derived poly α -olefin Group IV and refrigerant base oils. This approach provides a sustainable pathway for replacing petroleum-derived base oils.

Keywords: Lignin, Valorization, Biomass, Lubricants, hydroxyalkylation/alkylation, Hydrodeoxygenation, Renewable resources

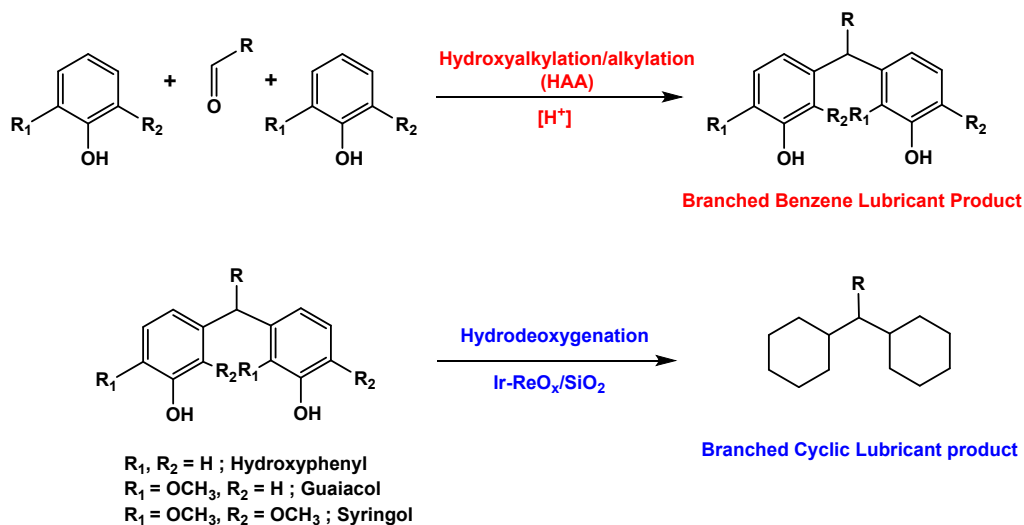
Introduction

Lubricants, representing an over \$126 billion global chemical enterprise¹, are essential to transportation, machinery, refrigeration compressors, and agricultural equipment. The projected market size by 2025 is \$183 billion². Base oils account for the majority of the lubricant cost and formulation (75-99% by weight). Synthetic base oils of lower viscosity, such as poly- α -olefins (PAOs), are typically used in automobiles, whereas higher viscosity base oils, like alkylbenzenes, in cooling and refrigeration, delivering better thermal stability, higher lubricity, and lower hygroscopicity than mineral oils for higher compressor temperatures^{3,4}. PAO and alkylbenzene lubricant base oils obtained from petroleum feedstocks contribute significantly to greenhouse gas emissions. Renewable alternatives can mitigate CO₂ emissions. Synthesis of high-performance biolubricant base oils can be impactful.

Biolubricant base oils produced from furans – one of the most widely studied biomass-derived platform chemicals, possess excellent performance⁵⁻⁸. Furans can be made from the carbohydrate fraction of biomass. Lignin is a naturally occurring crosslinked, functionalized biopolymer⁹⁻¹² composed of three main aromatic monomers (*p*-coumaryl, coniferyl, and sinapyl alcohol) linked via various C-C and C-O bonds. It is the only natural source of aromatic monomers^{13,14}. Presently, pulping and biorefining industries produce approximately 70-100 Mt/y isolated lignin^{15,16}. Most isolated lignins have a dark color, strong odor, broad molecular weight distribution, and limited reactivity^{12,15,17,18} due to high fractions of recalcitrant C-C bonds, relegating to low-value applications (*e.g.*, fillers for tires or burnt for energy)^{19,20}. Despite advances in lignin depolymerization to high-yield aromatic monomers^{10,21,22} (hydroxyphenols, guaiacols, and syringols), harnessing these platform monomers beyond pharmaceuticals^{10,13}, polymers²³, and fine chemicals²⁴ has received little attention.

We report a new strategy (Scheme 1) to synthesize (1) branched benzene lubricant (BBL) base oils *via* the hydroxyalkylation/alkylation (HAA) of lignin-derived guaiacol and lauryl aldehyde and (2) branched cyclic lubricant (BCL) base oils *via* the hydrodeoxygenation (HDO) of the BBL products. Our goal is to minimize the number of reaction steps needed to produce lubricant base oils while utilizing renewable and waste lignin derivatives and selective C-C hydroxyalkylation coupling chemistry. This approach contrasts the oligomerization of olefins to produce poly- α -olefins that is in general less selective in terms of controlling branching and molecular weight distribution and requires typically high energy for the production of olefins. BBL base oils possess

high viscosity and are used in cooling and refrigeration applications. BCL base oils are the saturated lubricant analogs with lower viscosity, typically used in automobile applications. We synthesized both BBL and BCL base oils to create two diverse product opportunities for applications in refrigeration and automobiles, respectively, to enhance the commercial strategy for market entry. A simple hydrogenation step converts BBL into BCL base oils in high yields (Scheme 1). While C–C coupling has been applied to upgrade furans into lubricants^{5,6}, application to lignin-derived monomers has rarely been exploited²⁵. Guaiacols are obtained either from woody or herbaceous biomass via reductive catalytic fractionation (RCF)^{10,23,26}. Aldehydes of varying carbon length can be synthesized via dehydrogenation of biomass-derived alcohols⁵ or selective hydrogenation of fatty acids from natural oils or waste cooking oils (WCO)²⁷. Optimum reaction conditions from guaiacol and lauryl aldehyde achieve a maximum guaiacol conversion of 90% with 76% BBL and 24% aldol condensation products over a P-SiO₂ catalyst. Subsequent HDO over an Ir-ReO_x/SiO₂ catalyst produces a lubricant-ranged mixture of BCL (C₂₄) at 82% yield and small fractions of dodecyl cyclohexane and C₁₀ and C₁₅ carbons alkanes. We characterize the product kinematic viscosity, viscosity index, and Noack volatility, finding comparable performance to petroleum-derived PAO, alkylbenzene, and cyclic alkane base oils.



Scheme 1: Strategy to produce branched benzene lubricant (BBL) base oils and branched cyclic lubricant (BCL) base oils via the HAA of lignin-derived monomers (hydroxyphenyls, guaiacols, and syringols) with an aldehyde and the HDO of the BBL product, respectively.

Materials and Methods

Materials

Aquivion PW98 [coarse powder, Brunauer-Emmett-Teller (BET) surface area $<1 \text{ m}^2/\text{g}$, and $1.0 \text{ mmol H}^+/\text{g}$], Nafion NR50 (pellets, BET surface area $<1 \text{ m}^2/\text{g}$, and $0.89 \text{ mmol H}^+/\text{g}$) (37), Amberlyst-15 (dry hydrogen form; pore size, 34.3 nm ; BET surface area, $42 \text{ m}^2/\text{g}$; and $4.8 \text{ mmol H}^+/\text{g}$), Pd/C ($10 \text{ wt}\%$ Pd loading), and sulphuric acid were purchased from Sigma-Aldrich. Amberlyst-36 dry resin (pore size, 32.9 nm ; BET surface area, $33 \text{ m}^2/\text{g}$; and $5.4 \text{ mmol H}^+/\text{g}$) (38) was purchased from the Rohm and Haas Company. Zeolite H β 12.5 (CP814e, Si/Al = 12.5) was purchased from Zeolyst and calcined before reaction. Silica gel (Fuji Silysia G-6) was purchased from Fuji silica. Silica gel (high-purity grade, pore size 60 \AA , 70-230 mesh) and H_2IrCl_6 containing $2.0976 \text{ wt}\%$ Iridium (Ir) were purchased from Sigma Aldrich, NH_4ReO_4 was purchased from Alfa Aesar, and Phosphoric acid ($85 \text{ wt}\%$) was purchased from Fisher chemical.

The P-SiO₂ catalyst (H_3PO_4 , $10 \text{ wt}\%$) was prepared by impregnation⁵. First, SiO₂ (high-purity grade, pore size 60 \AA , 70-230 mesh, Sigma-Aldrich) was impregnated with an aqueous H_3PO_4 solution. After evaporating the solvent at $75 \text{ }^\circ\text{C}$ on a hotplate and subsequently drying at $110 \text{ }^\circ\text{C}$ for 12 hr in an oven, the fine powder catalyst was calcined in a crucible in air at $500 \text{ }^\circ\text{C}$ for 3 hr with a $2 \text{ }^\circ\text{C}/\text{min}$ temperature ramp.

The Ir-ReO_x/SiO₂ (Ir, $4 \text{ wt}\%$; Re/Ir = 2) catalyst was prepared using sequential impregnation. First, Ir/SiO₂ was prepared by impregnating Ir on calcined SiO₂ (Fuji Silysia G-6, average pore diameter 6 nm , pore volume 0.7 ml/g) using 2- 3 drops of an aqueous solution of $63 \text{ wt}\%$ H_2IrCl_6 , mixing with a glass rod and crushing the lumps and drying. The process was repeated until all the aqueous solution of $63 \text{ wt}\%$ H_2IrCl_6 was exhausted. After evaporating the solvent at $75 \text{ }^\circ\text{C}$ on a hotplate for 2 hours (crushing the lumps every 15 minutes) and drying at $110 \text{ }^\circ\text{C}$ for 12 hr in an oven, the resulting Ir/SiO₂ was impregnated with ReO_x using 2- 3 drops of an aqueous solution of $3.7 \text{ wt}\%$ NH_4ReO_4 , mixing with a glass rod and crushing the lumps and drying. The process was repeated until all the aqueous solution of $3.7 \text{ wt}\%$ NH_4ReO_4 was exhausted. After evaporating the solvent at $75 \text{ }^\circ\text{C}$ on a hotplate for 2 hours (crushing the lumps every 15 minutes) and drying at $110 \text{ }^\circ\text{C}$ for 12 hr in an oven, the catalyst was calcined in a crucible in air at $500 \text{ }^\circ\text{C}$ for 3 hr with a $10 \text{ }^\circ\text{C}/\text{min}$ temperature ramp. The $4 \text{ wt}\%$ WO_x-Pt/C was prepared using the wet impregnation method^{28,29}. The reported metal loadings are based on the theoretical amount of metals in the precursor solution used in impregnation.

Guaiacol ($\geq 98.0\%$), 4-methyl guaiacol ($\geq 98.0\%$), 4-ethyl guaiacol ($\geq 98.0\%$), 4-propyl guaiacol ($\geq 99\%$), 2,6-dimethoxyphenol (99%), 4-methyl-2,6-dimethoxyphenol (97+%), phenol (99.0-100.5%), p-cresol ($\geq 99\%$), 4-ethylphenol (99%), 4-propylphenol (99%), lauryl aldehyde ($\geq 95\%$), and hexadecane (99%), were purchased from Sigma-Aldrich. Cyclohexane (99.9%) was purchased from Fisher Chemical.

Measurement of Reactivity and Selectivity

HAA reactions were performed in a Q-Tube™ Pressure Tube (Sigma Aldrich) reactor. In a typical reaction, 10 mmol (1.24 g) guaiacol and 5 mmol (0.92 g) lauryl aldehyde (without any solvent) were mixed in a 12-ml glass q-tube vial. The vial was placed in a preheated heating block and stirred at 500 rpm using a magnetic bar on a stirring hotplate. In the last step, the catalyst was added to the vial, and the reaction continued at the desired temperature for a specified reaction period. After the reaction, the q-tubes were cooled in an ice bath, and the solution was diluted using 10 ml of cyclohexane solvent. A small amount of hexadecane was added as an internal standard. For the recycle experiment, the recovered catalyst was washed thrice with cyclohexane and dried in air overnight. The spent (washed) catalyst was regenerated by calcination in air at 500 °C for 3 hr at a heating rate of 10 °C min⁻¹ before reuse.

For the semi-batch reactions, 1.25 mmol of lauryl aldehyde was added every 4 hr through an inlet valve connected to a syringe into the glass vial. This procedure was performed 4 times, yielding a total amount of 5 mmol, similar to the total lauryl aldehyde amount in the batch system.

The reaction mixture was transferred to a 20 ml centrifuge vial and centrifuged at 13500 × g for 5 min at 5 °C. The reaction mixture was then decanted into a new reactor with a fresh catalyst, and the deactivated (spent) P-SiO₂ catalyst was isolated for regeneration and thermogravimetric characterization.

HDO of BBLs over Ir-ReO_x/SiO₂ (and other catalysts) was performed in a 50-ml batch reactor (4790 pressure vessel, Parr Instrument Company) with an inserted Teflon liner and a magnetic stirrer. First, we added the catalyst (0.2 g) and solvent (10 ml of cyclohexane) to the reactor for catalyst prereduction and sealed the reactor with the reactor head equipped with a thermocouple, a rupture disk, a pressure gauge, and a gas release valve. The mixture was heated at 200 °C and 5 MPa H₂ for 1 hr at 240 rpm. Upon catalyst reduction, the reactor was cooled to room temperature, and the pressurized gases in the headspace were released. Then, we added BBLs (0.3 g) in a fume hood, closed the reactor head immediately, purged the reactor with 1 MPa H₂ three times,

pressurized to 5 MPa H₂, and heated it to the desired temperature under continuous stirring at 500 rpm. The set temperature was reached in about 25 min with a total pressure of ~6 MPa. Upon reaction, the reactor was immediately transferred to an ice bath. The reaction solution was diluted using 15 ml of cyclohexane with a small amount of hexadecane as an internal standard, and the catalyst was separated from the solution by filtration.

The products were analyzed using a gas chromatograph (GC, Agilent 7890A) equipped with an HP-1 column and a flame ionization detector using hexadecane (C₁₆) as an internal standard. The products were identified by a GC (Agilent 7890B) mass spectrometer (MS) (Agilent 5977A with a triple-axis detector) equipped with a DB-5 column, high-resolution MS with liquid injection field desorption ionization, ¹H nuclear magnetic resonance (NMR) (Bruker AV400, CDCl₃ solvent).

The conversion and the yield of all products were calculated on a carbon molar basis as follows

$$\text{Conversion [\%]} = \frac{\text{moles of initial reactant} - \text{moles of unreacted reactant}}{\text{moles of initial reactant}} \times 100 \quad (1)$$

$$\text{Yield of detected products [\%}_{-C}\text{]} = \frac{\text{moles}_{\text{product}} \times C \text{ atoms in product}}{\text{moles of total C atoms of guaiacol + lauryl aldehyde reactants}} \times 100 \quad (2)$$

The selectivity to each product is defined as follows.

$$\text{Selectivity}_{BBL} [\%] = \frac{\text{Yield}_{BBL}}{\text{Yield}_{BBL} + \text{Yield}_{\text{Enal byproduct}}} \times 100 \quad (3)$$

The reaction rates for forming BBL and enal byproduct were obtained at temperatures of 130, 140, and 150 °C. These values were then fit using an Arrhenius plot to obtain the apparent activation energy (E_a) for the products.

Thermogravimetric Analysis (TGA)

TGA was performed on fresh and spent P-SiO₂ catalysts using a TA instruments Q600 SDT thermogravimetric analyzer and differential scanning calorimeter (DSC) using a temperature program of 30 to 700 °C at a heating rate of 10 K min⁻¹ under air (30 mL min⁻¹).

Gas Composition Analysis

The gas component was analyzed using a MicroGC (990, Agilent) with a thermal conductivity detector (TCD). The MicroGC is equipped with four columns: 1 MS5A column with Ar carrier, 1 MS5A column, 1 PPU column, and 1 PPQ column with He carrier. The setup enables the detection

of H₂, He, N₂, CH₄, C₂H₆, C₂H₄, C₃H₆, C₃H₈, C₄H₈, CO, CO₂, and O₂ gases. N₂ gas was used to purge the MS detector for 20 min before feeding the sample.

Lubricant Properties

For the branched cyclic lubricant (BCL) product, cyclohexane was removed by rotary evaporation prior to viscosity measurements. The HAA product, containing BBL and enal byproduct, was characterized as-is (without further treatment). The properties of the synthesized base oils were evaluated according to the American Society for Testing and Materials (ASTM) methods. The kinematic viscosities at 100 ° and 40 °C (KV₁₀₀ and KV₄₀) were determined using the ASTM D445 method. The viscosity of the BCL product was measured using an extra-low-charge semi-micro viscometer (Cannon, size 150, calibrated model #: 9722-H62, calibrated with Cannon N35 Standard) apparatus⁸. The sample charge volume was 300 μL. The VI was calculated using the KV₁₀₀ and KV₄₀ following the ASTM D2270 method. All other measurements were performed at the Southwest Research Institute in San Antonio, Texas, USA. The Noack volatility was measured according to the ASTM D6375 method.

Results and Discussion

Hydroxyalkylation/alkylation (HAA) of Guaiacol and Lauryl Aldehyde

We evaluated different acid catalysts (Figure 1), including sulfonic acid resins, e.g., perfluorinated sulfonic acid resins (Aquivion PW98, Nafion NR50), sulfonic acid–functionalized crosslinked polystyrene resins (Amberlyst-15 and Amberlyst-36), commercial Hβ zeolite (CP814e), sulphuric acid, and phosphorous on silica (P-SiO₂) at equivalent acid amounts. The catalytic performance (evaluated based on the BBL yield) follows the order of P-SiO₂ > Nafion NR50 > Aquivion PW98 > H₂SO₄ > Amberlyst-15 > Amberlyst-36 > H-β (Figure 1). While homogenous acids, such as H₂SO₄, give good BBL yields, BBL product separation from the final solution containing acid becomes expensive and corrosion is a common challenge with homogeneous acids^{5-7,25}. Amongst the heterogenous catalysts, differences in BBL yield can be attributed to varying pore sizes which impact diffusion of reactive molecules to and from the catalytic active sites, the acid strength of the catalysts, and the adsorption strength around the catalytic site²⁵.

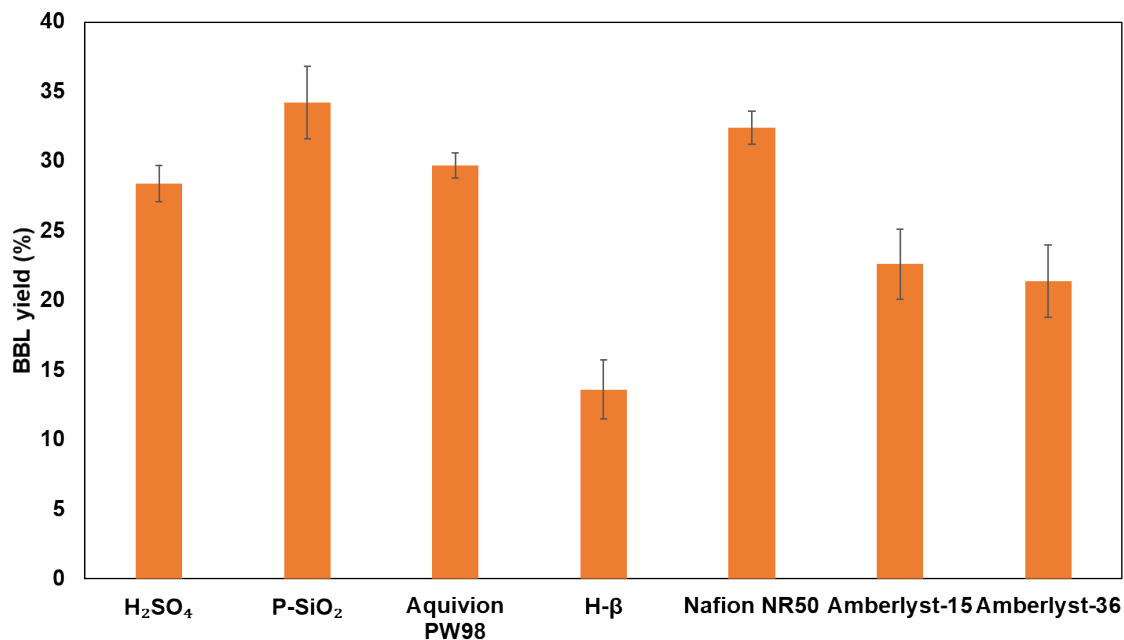


Figure 1: BBL yields in HAA reaction of guaiacol with lauryl aldehyde over various acid catalysts: 10 mmol guaiacol, 5 mmol lauryl aldehyde, and 0.05 mmol H⁺, 150 °C, 8 hr.

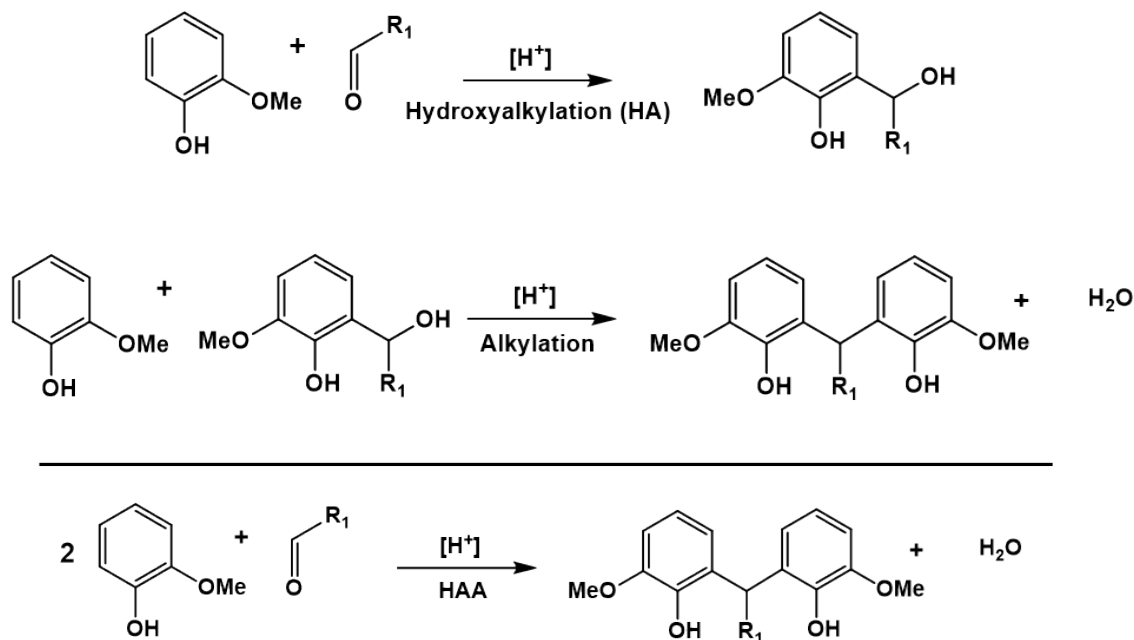
The mild HAA reaction conditions (65 °C, 6.5 hr, 50 mg P-SiO₂) used for the HAA of furan and aldehydes⁵ resulted in no products with a guaiacol feedstock. This is attributed to the electron-donation of the oxygen lone pair of electrons and excessive π electron density of the furan ring that makes it more reactive^{30–33}, especially for reactions involving an electrophilic aromatic substitution. Auto-condensation of the aldehyde was also observed, as reported elsewhere^{6,25,34–36} (Scheme 2). The enal product has the same number of carbons as the BBL and could also be used as a lubricant base oil. The GC–MS detected fragments at $m/z = 414$ and $m/z = 350.4$ (Figure S1) correspond to the BBL and aldol condensation enal product and their geometric isomers (e.g., meta-meta, meta-ortho, ortho-ortho dimers). ¹H NMR spectra (Figure S2) confirmed the reaction products identified via the GC–MS. We lumped all isomers of the same m/z fragment into a single product for yield calculations. Among the catalysts tested, P-SiO₂ gives the highest BBL yield and is amenable to regeneration, and was selected for the remaining of our work reported below.

Next, we investigated the effect of varying the P-SiO₂ amount, temperature, and reaction time on the HAA chemistry. We see a clear dependence on the reaction temperature (Figure S3), with 150 °C giving the highest BBL yield. Above 150 °C, there is no significant gain in lubricant yield at high conversions of reactants (Figure S3a). This halt in lubricant yield with increase in

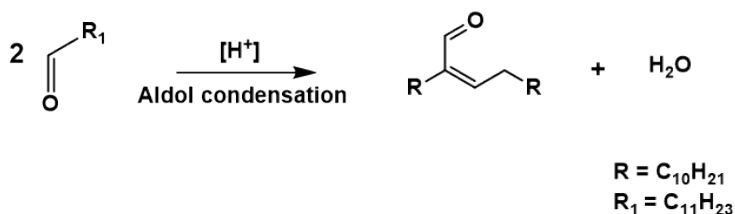
temperature can be attributed to P-SiO₂ deactivation as seen in recent literature^{5,25,37}. Figure S4 shows the increased conversions of guaiacol and lauryl aldehyde and the yield of BBL and enal byproduct with increasing the amount of P-SiO₂, as expected (Scheme 2).

Reaction 1 - HAA

Step 1 (HA) is the rate determining step



Reaction 2 - Aldol Condensation



Scheme 2: Stoichiometric equations for the HAA (the two individual steps and the total) and the aldol condensation reactions.

Heating lauryl aldehyde alone at 150 °C for 15 hr without P-SiO₂ catalyst led to enal product formation with 37% of lauryl aldehyde conversion resulting in a light-yellow solution (Figure S5). Upon adding the P-SiO₂ acid catalyst and repeating this experiment, all lauryl aldehyde was converted into the enal product, forming a dark-brown solution (Figure S5), further illustrating

that the P-SiO₂ catalyzes the aldol condensation reaction (Scheme 2). Achieving a higher BBL yield necessitates strategies to reduce this reaction. Above a P-SiO₂ loading of 150 mg, no significant increase in BBL yield, guaiacol, and lauryl aldehyde conversion is seen (Figure S4a). A 12 hr reaction time gave the highest BBL yield (Figure 2).

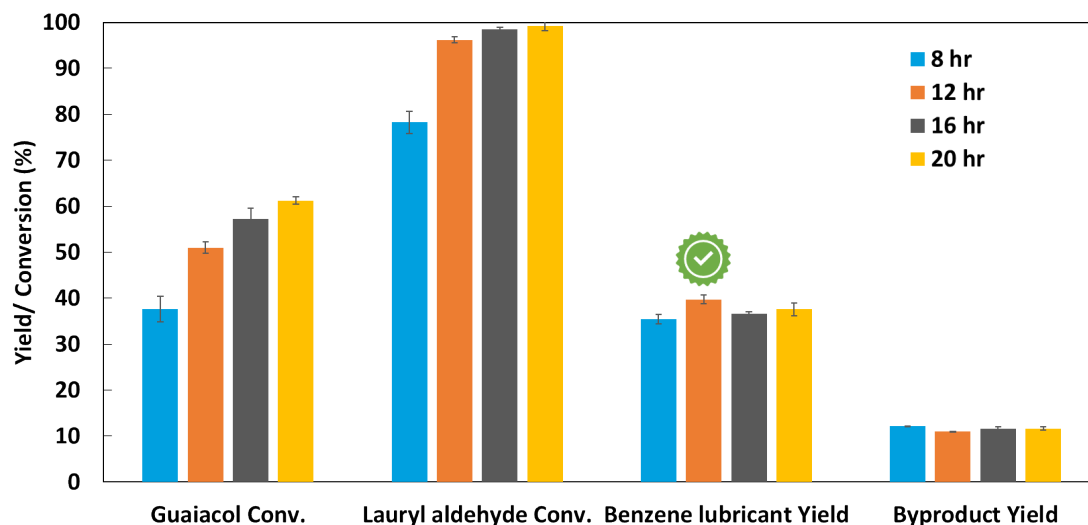


Figure 2: Effect of time on the yields of BBL and enal product and the conversion of guaiacol and lauryl aldehyde reactants. Reaction conditions: 10 mmol guaiacol, 5 mmol lauryl aldehyde, 150 °C, 150 mg P-SiO₂. Error bars denote standard deviation from triplicates.

Due to the relatively constant yield of BBL at the reaction times depicted in Figure 2, a time-dependent study at shorter reaction times was performed to understand the primary and secondary reactions taking place (Figure 3). Both HAA and aldol condensation reactions occur in parallel, affording BBL and enal product, respectively. Simultaneous lauryl aldehyde consumption in the parallel HAA and aldol condensation reactions explains its steeper consumption than guaiacol (Figure 2). The initial reaction rate data (Table S1) at various temperatures was used to estimate the apparent activation energies (E_a). E_a is 50 kJ mol⁻¹ for BBL and 72 kJ mol⁻¹ for the enal product. This difference in activation energies is due to different rate-determining steps in each reaction^{38,39}. Lower temperatures and longer reaction times promote selectivity.

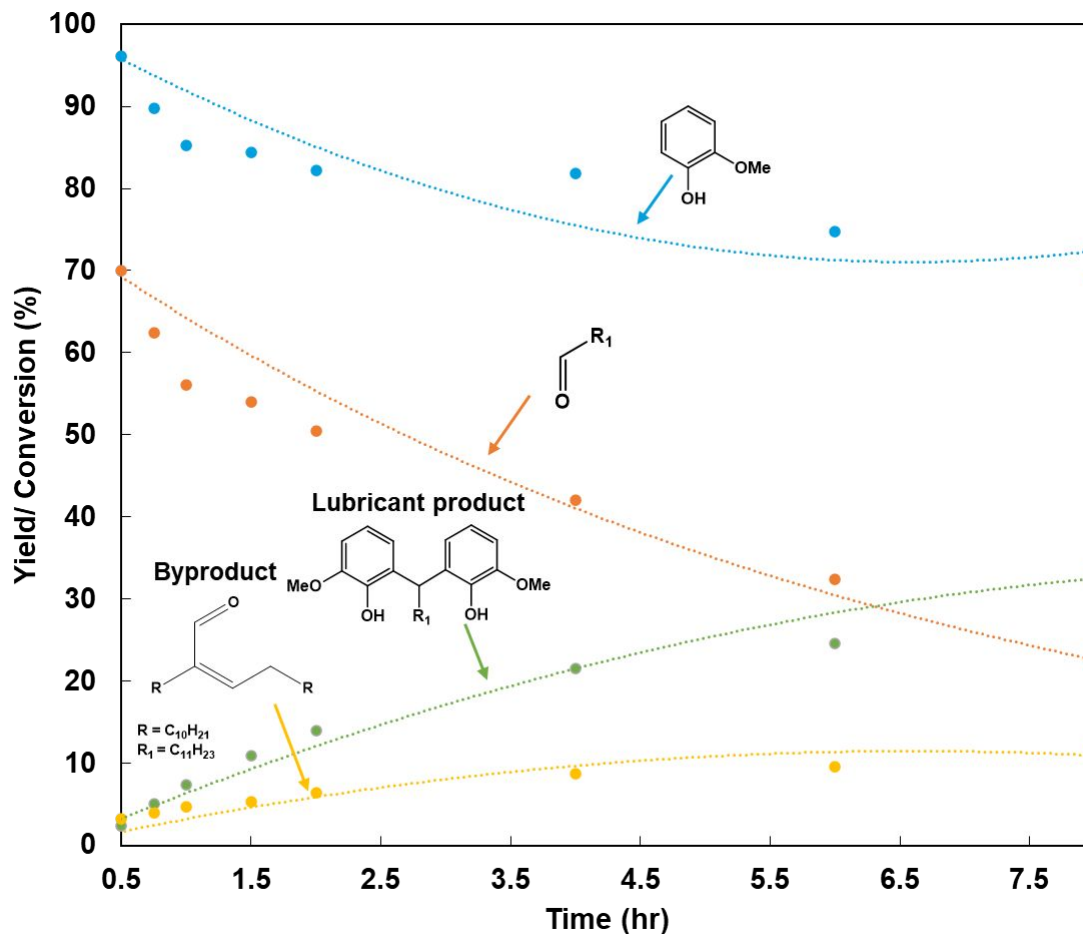


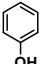
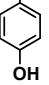
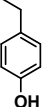
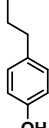
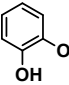
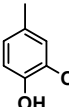
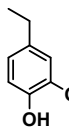
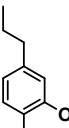
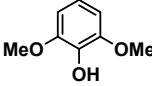
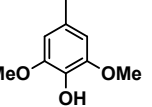
Figure 3: Time-dependent profile of hydroxyalkylation/alkylation (HAA) of guaiacol and lauryl aldehyde. Reaction conditions: 10 mmol guaiacol, 5 mmol lauryl aldehyde, 100 mg P-SiO₂, 150 °C. Carbon balance > 90 wt.%.

Optimal reaction conditions for the HAA reaction of guaiacol and lauryl aldehyde (150 °C, 150 mg P-SiO₂, 12 hr) afforded yields of ~40 wt.% BBL and ~11 wt.% enal product (Table S2). A semi-batch approach was adapted to minimize the enal product by periodically increasing the lauryl aldehyde in the reactor while providing the same total amount (see methods). As seen in Figure S6, reducing the loading of lauryl aldehyde in each period lowers the yield of condensation byproduct from 8.7 to 0.7 wt.% at 4 hr and increases the BBL yield to 54 wt.% with a selectivity of 87% to the BBL product (Table S2). Our results support that a semi-batch operation would limit the concentration of aldehyde and minimize the condensation (side) reaction. Increasing the reaction time or catalyst amount did not increase the guaiacol conversion beyond ~60 wt.% and led to poor carbon balance (<65%). We attributed this halt in guaiacol conversion to P-SiO₂

deactivation as seen in recent literature^{5,25,37}, which prevents further HAA reaction. TGA analysis of the spent catalyst showed significant mass loss compared to the fresh catalyst, attributed to oligomers and catalyst coking (Figure S7). GC analysis (Figure S8) of the washed spent catalysts in THF also indicated BBL adsorbed onto the spent catalyst. Coke forms rapidly (within the first minutes), changing the catalyst color from clear to dark brown/black (Figure S5). This observed catalyst deactivation can be remedied by regenerating the recovered catalyst. The spent catalyst was regenerated by (1) washing in cyclohexane thrice, next, (2) air-drying overnight, followed by (3) calcining of the washed and dried P-SiO₂ at 500 °C in air for 3 hr. The regenerated P-SiO₂ regained comparable performance to the fresh catalyst (Figure S9). To overcome the plateau in yield stemming from the catalyst deactivation halting the HAA reaction, the reaction mixture was separated from the deactivated catalyst after 12 hr by centrifugation and decantation, was transferred to a reactor with fresh catalyst, and reacted with additional lauryl aldehyde (stoichiometric amount based on unreacted guaiacol), leading to ~90 wt.% guaiacol conversion. The final HAA reaction product contained 76% BBL and 24% enal condensation product. These results support periodic or continuous catalyst regeneration in future work.

The HAA chemistry was exploited for several lignin-derived aromatic monomers (Table 1). Phenols give the highest conversion and selectivity to the BBL. This could be due to their smaller steric hindrance in the mesoporous P-SiO₂ catalyst than guaiacols and syringols. A small alkyl group (methyl, ethyl) in the phenol increased the conversion, likely due to the electron-donation of these groups activating the ring. Longer alkyl side chains (propyl) on the phenol negatively affect reactivity, probably due to steric effects^{5,25}. The presence of alkyl groups in guaiacols and syringols resulted in lower conversion and BBL selectivity. Methoxy and alkyl groups might sterically hinder the substrate from the catalyst sites and the lauryl aldehyde. Further work, including reactant and product transport limitations in heterogeneous catalysts with varying pore size, would be worthy for understanding these trends better.

Table 1: HAA data of several lignin-derived phenolic substrates.

Substrate	Conversion (%)	Laurylaldehyde conversion (%)	BBL Yield (Selectivity)* (%)
Phenol	 67	99.8	63 (91)
Methyl phenol	 70	99.8	68 (93)
Ethyl phenol	 72	99.8	68 (95)
Propyl phenol	 65	93.3	61 (86)
Guaiacol	 51	96.2	40 (78)
Methyl guaiacol	 38	91.4	31 (64)
Ethyl guaiacol	 33	83.2	23 (43)
Propyl guaiacol	 20	55.4	14 (38)
Syringol	 52	87.4	34 (67)
Methyl syringol	 11	50.2	0 (0)

*Reaction products: BBL and enal byproduct. Carbon balance > 85 wt.% (HA intermediate is added in the balance).

Reaction conditions: 10 mmol substrate, 5 mmol lauryl aldehyde, 150 °C, 12 hr, 150 mg P-SiO₂

HDO to Cyclic and Branched-alkane Base Oils

The BBL and enal HAA reaction product was dissolved in cyclohexane and transferred to a Parr reactor for HDO. We adapted conditions employed in the production of jet fuels⁴⁰ and lubricants^{5–8} and optimized them. Ir-ReO_x/SiO₂ was selected due to its excellent HDO performance reported in our previous works^{5–8,40}. This group of metal/metal oxide catalysts has been used successfully also for ring opening of saturated furans to diols and hydrogenolysis of other substrates, such as glycerol^{28,41–46}. At 180 °C used in prior works^{5,8}, there remains unconverted BBL and enal byproduct (Figure 4), suggesting higher reaction temperature and/or longer reaction times for complete HDO. At 200 °C, the BBL and enal byproduct are fully converted into cyclic C₂₄ alkane and branched aliphatic C₂₄ lubricant products, respectively, given the complete disappearance of the BBL (peaks at ~20–20.5 mins) and enal byproduct (peaks at ~17.6 mins), respectively (Figure 4). ¹H NMR spectra after HDO (Figure S10) corroborate the complete disappearance of aromatic signals (chemical shift 6.5 – 6.8 ppm) and consistency with the GC–MS data (Figure S11). At ≥ 220 °C, BBL and enal byproduct are completely converted but also more C–C cracking products to dodecyl cyclohexane (peak at ~13.5 mins) and shorter chain branched lubricants (side peaks between ~15 – 15.5 mins), respectively. 200 °C was used for subsequent HDO experiments to minimize cracking while ensuring complete conversion.

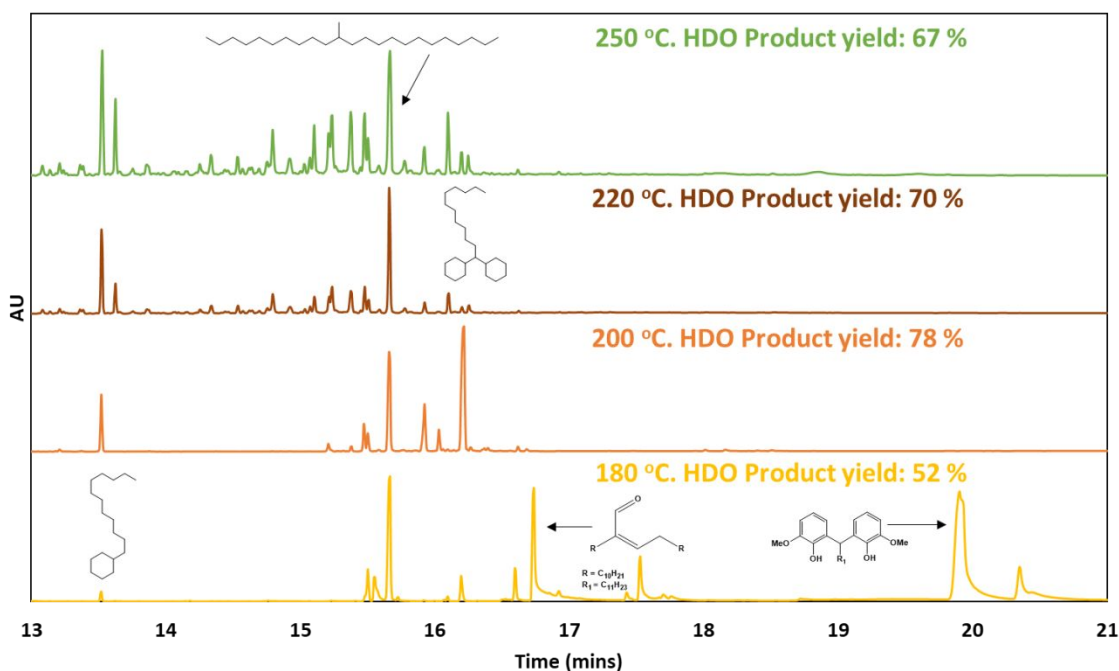


Figure 4: GC profile of HDO over Ir-ReO_x catalyst at different temperatures (0.3 g HAA reaction product, 0.2 g Ir-ReO_x on silica, 20 ml cyclohexane, 500 rpm, 18 hr, 5 MPa H₂).

At 200 °C, a reaction time of 6 hr was insufficient for complete HDO; 12 hr gave the highest lubricant yield (82%). Longer reaction times led to more C-C cracking and lower lubricant yields (Figure S12). Other HDO catalysts (Pd/C and 4 wt.% WO_x-Pt/C) afforded lower HDO lubricant yields (Figure S13). The optimized reaction conditions afforded a lubricant mixture of 82% cyclic C₂₄ alkane and branched aliphatic C₂₄ base oil, with a distinct chromatogram (Figure 5) from the HAA reaction product. GC analysis of the gas phase after HDO identified light alkanes (C₂H₆, C₃H₈, C₄H₈) from C-C cracking reactions. Small fractions of dodecyl cyclohexane and small alkanes from C-C cracking are also observed in the liquid phase. Notably, our biobased lubricant base oils form selectively, minimizing expensive and complex separations associated with commercial mineral and synthetic base oils. A summary of all HDO results is in Table S3.

Under similar reaction conditions, Pd/C still left oxygenated products. WO_x-Pt/C cracked the branched cyclic lubricant product, reducing the C₂₄ alkane lubricant yield, likely due to the strong acidity of the catalyst. The excellent performance of the Ir-ReO_x catalyst for HDO arises from a synergy between Ir and ReO_x sites, whereby the Ir sites hydrogenate the benzene rings, and the acidic sites of ReO_x activate the C-O bonds of the methoxy and phenolic groups. Selective HDO of lignin derivatives (phenols, cresols, and guaiacols) over metal/metal oxide catalysts has been demonstrated in recent works^{29,47,48}. To our knowledge, HDO and ring hydrogenation over these catalysts has not been reported before. Further simultaneous optimization of operating conditions and catalysts could further increase the yield for practical implementation.

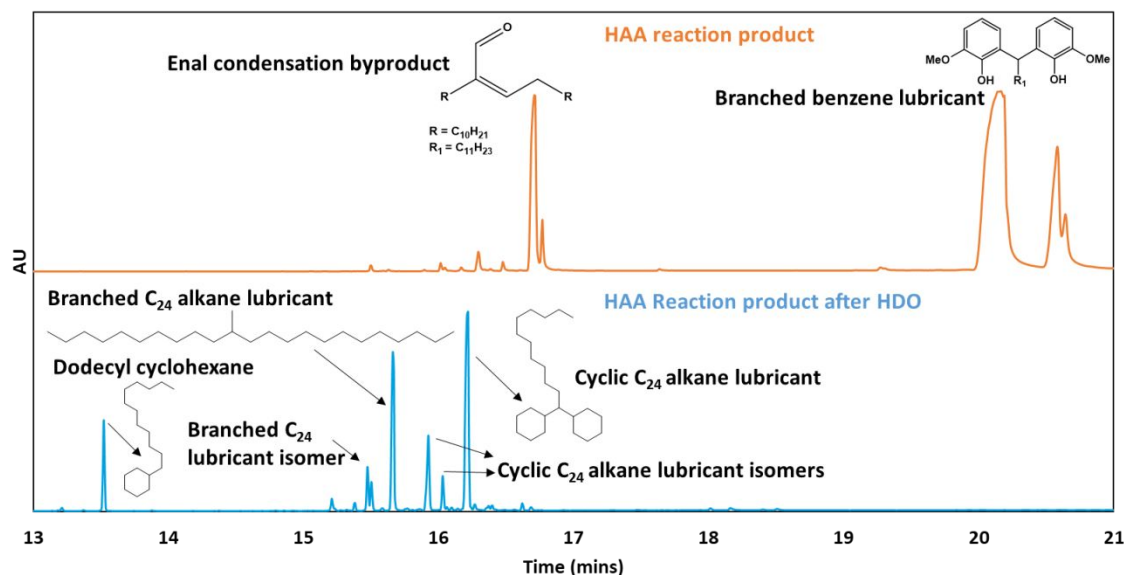


Figure 5: GC chromatogram of HAA reaction product before (top) and after (bottom) HDO (0.3 g HAA reaction product, 0.2 g Ir-ReOx on silica, 20 ml cyclohexane, 500 rpm, 200 °C, 12 hr, 5 MPa H₂).

Lubricant properties

Our HAA BBL and enal condensation product is a highly viscous and dark-amber colored liquid at room temperature. After HDO, the obtained lubricant oil is less viscous and clear (Figure S14). Important properties (kinematic viscosity, VI, and Noack volatility) of the base oils are compared with commercial mineral and alkylbenzene base oils, categorized by the American Petroleum Institute in Table 2. Lubricant base oils should have high viscosities at high temperatures to create a thick hydrodynamic film between surfaces. At lower temperatures, base oils should be less resistant to flow, promoting fluidity. The viscosity index (VI), calculated using the KV₁₀₀ and KV₄₀ values, indicates the change in viscosity with temperature. A high viscosity index (VI) ensures lower dependence of lubricant viscosity on temperature, which is desirable for the lubricating film operating over a wide temperature range. Table 2 shows that the KV₁₀₀ and KV₄₀ of our base oils are comparable to commercial Group III, IV and refrigerant base oils. The VI of our lubricant mix of cyclic and branched C₂₄ alkane base oil is above 100, indicating good lubricant quality.

Table 2. Properties of HAA reaction product and lubricant mix of cyclic and branched C₂₄ alkane base oil compared with those of select commercial lubricants.

Base oil	KV ₁₀₀ (cSt)	KV ₄₀ (cSt)	VI	Noack Volatility (wt.%)
C ₂₄ lubricant product mix	3.18	12.6	118	37.10
ExxonMobil PAO4	4.1	19.0	126	18.80
Exxon Mobil SpectraSyn Plus PAO-3.6	3.6	15.4	120	< 17.0
HAA reaction product	12.2	238	-31	16.30
Mobil EAL Arctic 220	18.1	220	88	-

The properties of commercial products were obtained from the product specifications datasheet disclosed by the manufacturers. HAA reaction product contains 76% BBL and 24% enal product. The C₂₄ lubricant product mix contains 62% branched cyclic lubricant, 22% branched lubricant, 12% dodecyl cyclohexane, and 4% alkanes.

The high viscosity of the HAA reaction product could be due to aromaticity, molecular structure, and oxygen in the phenolic and methoxy groups. These hydrophilic groups improve the polarity of base oils and enhance their solubility with polar additives for refrigerant applications³. At higher temperatures, the viscosity of the HAA reaction product drops significantly, resulting in a negative viscosity index. This implies that the HAA reaction product rapidly thickens with decreasing temperature and thins out with increasing temperature. The high Noack volatility of the C₂₄ lubricant mix is attributed to the lighter hydrocarbon fragments in the base oil mix that evaporate under testing conditions. Conversely, the HAA reaction product has better volatility compared to commercial lubricants as it consists of high boiling point components.

Conclusions

We demonstrated a new route to branched benzene lubricant (BBL) and branched cyclic lubricant (BCL) base oils from lignin-derived monomer guaiacol and fatty acid-derived aldehydes, such as lauryl aldehyde, using hydroxyalkylation/alkylation (HAA) followed by hydrodeoxygenation (HDO). The main products of the HAA step were BBL and an aldol condensation enal product with a carbon balance of >85 wt.%. A semi-batch operation was introduced, affording ~90 wt.% guaiacol conversion and final HAA reaction product composition

of 76% BBL and 24% enal condensation product at optimal reaction conditions (150 °C, 150 mg P-SiO₂, 12 hr). This strategy can be extended to other lignin-related substrates, with activity and selectivity varying depending on functional groups and size. Subsequent HDO over an Ir-ReO_x/SiO₂ catalyst (Re/Ir molar ratio = 2) yielded 82% lubricant-ranged C₂₄ cyclic and branched alkanes base oils. Viscosity measurements indicate viscous properties comparable to petroleum-derived Group III, IV, and refrigerant base oils. This strategy to synthesize renewable base oils could replace petroleum-derived base oils and reduce the carbon footprint.

Acknowledgments

This work was supported as part of the Catalysis Center for Energy Innovation, an Energy Frontier Research Center funded by the U.S. Department of Energy, Office of Science, and Office of Basic Energy Sciences under award number DE-SC0001004. E.E. also acknowledges support from the Delaware Environmental Institute Fellows Program from the University of Delaware.

Competing interests: The authors are inventors on a patent application on the process described in the manuscript.

Data and materials availability

All data needed to evaluate the conclusions in the paper are in the paper and/or the Supplementary Materials. Additional data regarding this paper may be requested from the authors.

References

- 1 G. V. Research, Lubricants Market Size, Share | Industry Report, 2021-2028, <https://www.grandviewresearch.com/industry-analysis/lubricants-market>, (accessed 13 April 2021).
- 2 C. P. Newswire, The global lubricants market size is projected to reach USD 182.6 billion by 2025 from USD 157.6 billion in 2020, at a CAGR of 3.0%, <https://www.prnewswire.com/news-releases/the-global-lubricants-market-size-is->

- projected-to-reach-usd-182-6-billion-by-2025-from-usd-157-6-billion-in-2020--at-a-cagr-of-3-0-301096072.html, (accessed 13 April 2021).
- 3 K. Takigawa, S. I. Sandler and A. Yokozeki, *Int. J. Refrig.*, 2002, **25**, 1014–1024.
 - 4 W. D. Cooper, R. C. Downing and J. B. Gray, *Alkyl Benzene as a Compressor Lubricant*, Wilmington, 1974.
 - 5 S. Liu, T. R. Josephson, A. Athaley, Q. P. Chen, A. Norton, M. Ierapetritou, J. I. Siepmann, B. Saha and D. G. Vlachos, *Sci. Adv.*, 2019, **5**, 1–8.
 - 6 S. Liu, B. Saha and D. G. Vlachos, *Green Chem.*, 2019, **21**, 3606–3614.
 - 7 S. Liu, R. Bhattacharjee, S. Li, A. Danielson, T. Mazal, B. Saha and D. G. Vlachos, *Green Chem.*, 2020, **22**, 7896–7906.
 - 8 A. M. Norton, S. Liu, B. Saha and D. G. Vlachos, *ChemSusChem*, 2019, **12**, 4780–4785.
 - 9 S. Van Den Bosch, W. Schutyser, R. Vanholme, T. Driessen, S. F. Koelewijn, T. Renders, B. De Meester, W. J. J. Huijgen, W. Dehaen, C. M. Courtin, B. Lagrain, W. Boerjan and B. F. Sels, *Energy Environ. Sci.*, 2015, **8**, 1748–1763.
 - 10 O. E. Ebikade, N. Samulewicz, S. Xuan, J. D. Sheehan, C. Wu and D. G. Vlachos, *Green Chem.*, 2020, **22**, 7435–7447.
 - 11 Y. M. Questell-Santiago, M. V Galkin, K. Barta and J. S. Luterbacher, *Nat. Rev. Chem.*, , DOI:10.1038/s41570-020-0187-y.
 - 12 R. M. O’dea, J. A. Willie and T. H. Epps, *ACS Macro Lett.*, 2020, **9**, 476–493.
 - 13 S. Elangovan, A. Afanasenko, J. Hauptenthal, Z. Sun, Y. Liu, A. K. H. Hirsch and K. Barta, *ACS Cent. Sci.*, 2019, **5**, 1707–1716.
 - 14 J. Gierer, *Wood Sci. Technol.*, 1985, **19**, 289–312.
 - 15 D. S. Bajwa, G. Pourhashem, A. H. Ullah and S. G. Bajwa, *Ind. Crops Prod.*, 2019, **139**, 111526.
 - 16 L. Dessbesell, M. Paleologou, M. Leitch, R. Pulkki and C. (Charles) Xu, *Renew. Sustain. Energy Rev.*, 2020, **123**, 109768.
 - 17 O. Ajao, J. Jeaidi, M. Benali, A. Restrepo, N. El Mehdi and Y. Boumghar, *Molecules*, 2018, **23**, 377.
 - 18 O. Ajao, J. Jeaidi, M. Benali, O. Y. Abdelaziz and C. P. Hulteberg, *Bioresour. Technol.*, , DOI:10.1016/j.biortech.2019.121799.
 - 19 *Chem. Eng. News*, 1957, **35**, 28–30.

- 20 C. L. Chambon, M. Chen, P. S. Fennell and J. P. Hallett, *Front. Chem.*, 2019, **7**, 246.
- 21 L. Shuai, M. T. Amiri, Y. M. Questell-Santiago, F. Héroguel, Y. Li, H. Kim, R. Meilan, C. Chapple, J. Ralph and J. S. Luterbacher, *Science*, 2016, **354**, 329–334.
- 22 E. M. Anderson, M. L. Stone, R. Katahira, M. Reed, G. T. Beckham and Y. Román-Leshkov, *Joule*, 2017, **1**, 613–622.
- 23 S. Wang, L. Shuai, B. Saha, D. G. Vlachos and T. H. Epps, *ACS Cent. Sci.*, 2018, **4**, 701–708.
- 24 Y. Liao, S. F. Koelewijn, G. van den Bossche, J. van Aelst, S. van den Bosch, T. Renders, K. Navare, T. Nicolai, K. van Aelst, M. Maesen, H. Matsushima, J. M. Thevelein, K. van Acker, B. Lagrain, D. Verboekend and B. F. Sels, *Science (80-.)*, 2020, **367**, 1385–1390.
- 25 P. Ferrini, S. F. Koelewijn, J. Van Aelst, N. Nuttens and B. F. Sels, *ChemSusChem*, 2017, **10**, 2249–2257.
- 26 S. Sadula, N. Rodriguez Quiroz, A. Athaley, O. E. Ebikade, M. Ierapetritou, D. Vlachos and B. Saha, *Green Chem.*, 2021, **23**, 1200–1211.
- 27 T. Yokoyama and N. Yamagata, *Appl. Catal. A Gen.*, 2001, **221**, 227–239.
- 28 C. Wang, J. D. Lee, Y. Ji, T. M. Onn, J. Luo, C. B. Murray and R. J. Gorte, *Catal. Letters*, 2018, **148**, 1047–1054.
- 29 C. Wang, A. V. Mironenko, A. Raizada, T. Chen, X. Mao, A. Padmanabhan, D. G. Vlachos, R. J. Gorte and J. M. Vohs, *ACS Catal.*, 2018, **8**, 7749–7759.
- 30 K. E. Horner and P. B. Karadakov, *J. Org. Chem.*, 2013, **78**, 8037–8043.
- 31 P. Kumar, M. Varkolu, S. Mailaram, A. Kunamalla and S. K. Maity, in *Polygeneration with Polystorage: For Chemical and Energy Hubs*, Elsevier, 2018, pp. 373–407.
- 32 N. Barthel, A. Finiels, C. Moreau, R. Jacquot and M. Spagnol, *J. Mol. Catal. A Chem.*, 2001, **169**, 163–169.
- 33 G. M. Loudon, in *Organic Chemistry*, 5th edn., 2009, pp. 1–1374.
- 34 H. A. Meylemans, T. J. Groshens and B. G. Harvey, *ChemSusChem*, 2012, **5**, 206–210.
- 35 S. Zhao and M. M. Abu-Omar, *ACS Sustain. Chem. Eng.*, 2016, **4**, 6082–6089.
- 36 M. Balakrishnan, G. E. Arab, O. B. Kunbargi, A. A. Gokhale, A. M. Grippo, F. D. Toste and A. T. Bell, *Green Chem.*, 2016, **18**, 3577–3581.
- 37 H. J. Cho, M. J. Kuo, M. Ye, Y. Kurz, Y. Yuan and R. F. Lobo, *ACS Sustain. Chem. Eng.*, 2021, acssuschemeng.0c09227.

- 38 G. Li, N. Li, Z. Wang, C. Li, A. Wang, X. Wang, Y. Cong and T. Zhang, *ChemSusChem*, 2012, **5**, 1958–1966.
- 39 A. N. Migués, S. Vaitheeswaran and S. M. Auerbach, *J. Phys. Chem. C*, 2014, **118**, 20283–20290.
- 40 S. Liu, T. Simonetti, W. Zheng and B. Saha, *ChemSusChem*, 2018, **11**, 1446–1454.
- 41 S. Koso, I. Furikado, A. Shima, T. Miyazawa, K. Kunimori and K. Tomishige, *Chem. Commun.*, 2009, 2035–2037.
- 42 Y. Nakagawa and K. Tomishige, *Catal. Today*, 2012, **195**, 136–143.
- 43 B. Xiao, M. Zheng, X. Li, J. Pang, R. Sun, H. Wang, X. Pang, A. Wang, X. Wang and T. Zhang, *Green Chem.*, 2016, **18**, 2175–2184.
- 44 J. He, S. P. Burt, M. Ball, D. Zhao, I. Hermans, J. A. Dumesic and G. W. Huber, *ACS Catal.*, 2018, **8**, 1427–1439.
- 45 E. Soghrati, C. Kok Poh, Y. Du, F. Gao, S. Kawi and A. Borgna, *ChemCatChem*, 2018, **10**, 4652–4664.
- 46 K. J. Stephens, A. M. Allgeier, A. L. Bell, T. R. Carlson, Y. Cheng, J. T. Douglas, L. A. Howe, C. A. Menning, S. A. Neuenswander, S. K. Sengupta, P. S. Thapa and J. C. Ritter, *ACS Catal.*, 2020, **10**, 12996–13007.
- 47 R. Shu, R. Li, B. Lin, C. Wang, Z. Cheng and Y. Chen, *Biomass and Bioenergy*, 2020, 132, 105432.
- 48 Y. Jing and Y. Wang, *Front. Chem. Eng.*, 2020, **2**, 10.